Brian D. Stemper¹

e-mail: bstemper@mcw.edu

Steven G. Storvik Narayan Yoganandan

Department of Neurosurgery,
Medical College of Wisconsin,
Milwaukee, WI 53226
Department of Biomedical Engineering,
Marquette University,
Milwaukee, WI 53201
Veterans Affairs Medical Center,
Milwaukee, WI 53295

Jamie L. Baisden

Department of Neurosurgery, Medical College of Wisconsin, Milwaukee, WI 53226; Veterans Affairs Medical Center, Milwaukee, WI 53295

Ronald J. Fijalkowski

Department of Neurosurgery, Medical College of Wisconsin, Milwaukee, WI 53226

Frank A. Pintar

Department of Neurosurgery,
Medical College of Wisconsin,
Milwaukee, WI 53226;
Department of Biomedical Engineering,
Marquette University,
Milwaukee, WI 53201;
Veterans Affairs Medical Center,
Milwaukee, WI 53295

Barry S. Shender Glenn R. Paskoff

Naval Air Warfare Center Aircraft Division, Patuxent River, MD 20670

A New PMHS Model for Lumbar Spine Injuries During Vertical Acceleration

Ejection from military aircraft exerts substantial loads on the lumbar spine. Fractures remain common, although the overall survivability of the event has considerably increased over recent decades. The present study was performed to develop and validate a biomechanically accurate experimental model for the high vertical acceleration loading to the lumbar spine that occurs during the catapult phase of aircraft ejection. The model consisted of a vertical drop tower with two horizontal platforms attached to a monorail using low friction linear bearings. A total of four human cadaveric spine specimens (T12-L5) were tested. Each lumbar column was attached to the lower platform through a load cell. Weights were added to the upper platform to match the thorax, head-neck, and upper extremity mass of a 50th percentile male. Both platforms were raised to the drop height and released in unison. Deceleration characteristics of the lower platform were modulated by foam at the bottom of the drop tower. The upper platform applied compressive inertial loads to the top of the specimen during deceleration. All specimens demonstrated complex bending during ejection simulations, with the pattern dependent upon the anterior-posterior location of load application. The model demonstrated adequate inter-specimen kinematic repeatability on a spinal level-by-level basis under different subfailure loading scenarios. One specimen was then exposed to additional tests of increasing acceleration to induce identifiable injury and validate the model as an injuryproducing system. Multiple noncontiguous vertebral fractures were obtained at an acceleration of 21 g with 488 g/s rate of onset. This clinically relevant trauma consisted of burst fracture at L1 and wedge fracture at L4. Compression of the vertebral body approached 60% during the failure test, with -6,106 N axial force and 168 Nm flexion moment. Future applications of this model include developing a better understanding of the vertebral injury mechanism during pilot ejection and developing tolerance limits for injuries sustained under a variety of different vertical acceleration scenarios.

[DOI: 10.1115/1.4004655]

1 Introduction

Military ejection seats are designed to egress the aviator from the aircraft in the event of an imminent crash. These vital safety devices exert substantial axial loads on the spinal column during the catapult phase as the seat must vertically displace the pilot over a very short time period to avoid contacting posterior structures of the aircraft. The spinal column is forced to bear this load with the caudal extent carrying the maximum share. Early ejection seat accelerations approached the level of human tolerance, which

¹Corresponding author.

was reflected by fatality rates exceeding 17% [1,2]. However, an improved understanding of human tolerance limits has led to more survivable aircraft ejection events, with contemporary fatality rates commonly reported to be well below 10% [3–7]. As the survivability of aircraft ejection has increased, the focus has turned toward injury prevention. Extreme loads experienced by the spinal column during ejection commonly result in vertebral fractures. Large-scale clinical studies have reported vertebral fracture rates of 14% to 35% [3,6–10]. These fractures commonly affect the thoraco-lumbar spine. Therefore, an improved understanding of the dynamic biomechanics of the lumbar spine is required to advance the level of aviator safety during aircraft ejection.

Previous laboratory-based experimentation has investigated dynamic lumbar spine tolerance under compressive or compression-flexion loading using post-mortem human subjects (PMHS) or bovine spines. Those studies typically involved fixing the caudal end of the specimen and applying a vertical load to the cranial end using weight-drop [11–17] or MTS piston [18–24] techniques.

Journal of Biomechanical Engineering

AUGUST 2011, Vol. 133 / 081002-1

Contributed by the Bioengineering Division of ASME for publication in the JOUR-NAL OF BIOMECHANICAL ENGINEERING. Manuscript received November 18, 2010; final manuscript received July 8, 2011; published online August 30, 2011. Assoc. Editor: Beth Winkelstein.

This material is declared a work of the US Government and is not subject to copyright protection in the United States. Approved for public release; distribution is unlimited.

The models were used to investigate vertebral fracture mechanisms and characteristics. Although they provided clinically relevant data and tolerance thresholds in terms of forces and moments, the models have drawbacks for fully characterizing the injury mechanism. For example, the caudal end of the specimen was rigidly fixed to the testing apparatus. While this boundary condition is experimentally expedient, it does not replicate the acceleration-driven loading applied to the pelvis during real-world vertical acceleration scenarios such as military pilot ejection or falls from height. Therefore, characteristics of the acceleration versus time pulse at the base of the spine, such as maximum acceleration, duration, and rate of onset, cannot be related to the presence/absence or type of vertebral fracture produced during the test. These characteristics are important in producing clinically relevant injury types and severities, defining injury tolerance thresholds, and designing improved safety devices (e.g., ejection seats) [12]. The MTS piston technique is limited in terms of the range of pulse characteristics by machine specifications, and the weight-drop method has not exhibited flexibility in the magnitude or shape of acceleration pulses in its current form, only reporting blunt-impact accelerations.

To fully understand injury mechanisms and characteristics of a pilot ejection, an archetypal axial loading scenario, a biomechanically accurate and repeatable model capable of quantifying metrics associated with injury tolerance (i.e., accelerations, loads, kinematics) must be used. Thus, the current study focused on the development of a test methodology that would accurately quantify experimental response corridors of the PMHS thoracolumbar

spine under dynamic axial loading using realistic boundary conditions.

2 Methods

The experimental model was designed to simulate loads sustained by the lumbar spine during high rate vertical acceleration as experienced during pilot ejection or falls from height. Four lumbar spine specimens (T12 to L5) were obtained from PMHS donors aged 25 to 46 years. PMHS were screened such that height and weight approximated the demographics of Naval aviators. Spines were cleaned of muscular and surrounding tissue, leaving only vertebrae, ligaments, and intervertebral discs intact. Lumbar spines were fixed at cranial and caudal ends using polymethylmethacrylate (PMMA) to facilitate attachment to the loading device. The L2-L3 intervertebral disc was maintained horizontal during the fixation procedure to control the initial position in the absence of any good precedent. CT scans were taken for pre- and post-test comparison of the bony vertebral geometry (Siemens, Malvern, PA).

The loading device consisted of two horizontal platforms attached to a 13-mm diameter stainless steel monorail using low friction precision linear steel bearings. The monorail was vertically supported by a 7.6-m high drop tower which has been previously described [25]. A stabilizing outrigger bearing mechanism prevented rotation of the platforms about the vertical axis. The two platforms were connected to each other using a cable that allowed the upper platform to compress the specimen while limiting relative displacement beyond the initial vertical distance

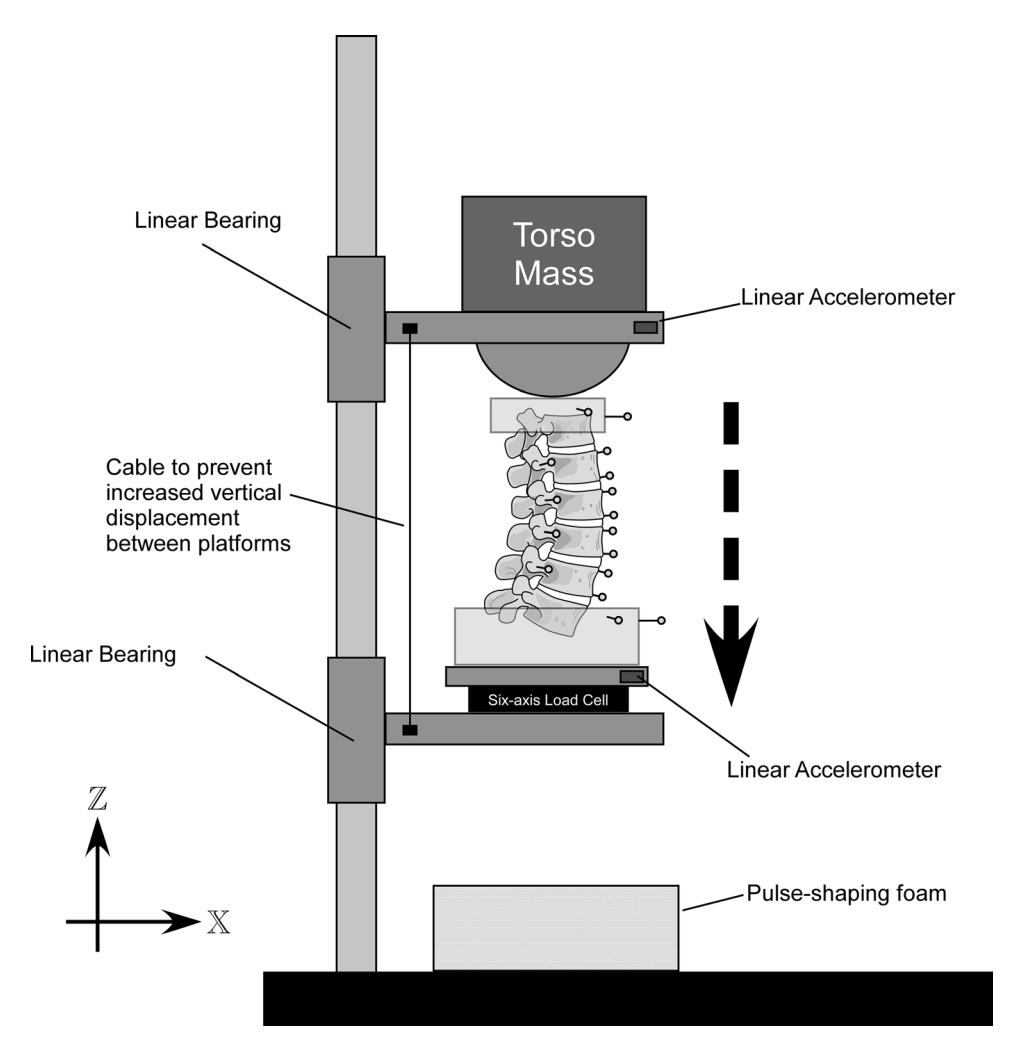


Fig. 1 Lumbar spine vertical acceleration model. Axes for coordinate systems follow the right hand rule.

081002-2 / Vol. 133, AUGUST 2011

Transactions of the ASME

between the two platforms (Fig. 1). The specimen was attached to the lower platform through a six-axis load cell (Robert A. Denton Inc., Rochester, MI) with the following values for maximum range: shear force ±4448 N, axial force ±8896 N, bending ±565 Nm, and twist ± 339 Nm. The load cell was centered in the axial plane at approximately the posterior aspect of the L3 vertebral body. Uniaxial accelerometers (± 2000 g, Endevco Corp., San Juan Capistrano, CA) were attached to upper and lower platforms and oriented to record vertical acceleration. Variable weight could be attached to the upper platform to simulate mass of the torso, head-neck, and upper extremities. Interaction between the upper platform and the superior PMMA fixation was in the form of a laterally oriented cylinder. Slippage was prevented by wrapping the cylinder in gauze and placing compressed foam on the rostral surface of the PMMA fixation. A lack of slippage was videographically confirmed following each test. The impacting cylinder was attached to the upper platform through a telescoping linkage, such that compressive loads could be applied in a variety of anteroposterior positions relative to the cranial end of the specimen.

Specimens were oriented in the initial position prior to raising the test rig, consisting of both platforms, instrumentation, and the specimen, to the drop height. The test rig was held in place using a high-power magnet. Initial position was maintained by placing the cylinder of the upper platform in contact with the superior fixation of the specimen. Relative positioning of the two platforms was maintained by a cable that prevented increasing distance. Therefore, specimens were supported from the lower platform prior to impact and not suspended from the upper platform. Upon manual trigger, power to the magnet was removed and the apparatus was accelerated downward by gravity until contacting the pulse-shaping foam at the bottom of the drop tower. The foam dimensions were $30 \times 45 \times 65$ cm (X,Y,Z) and had a density of 16 kg/m^3 . The compressive mechanical properties are provided in Fig. 2. Because upper and lower platforms were decoupled, the upper platform applied a compressive inertial load to the top of the specimen as the lower platform decelerated due to contact with the foam. The acceleration pulse of the lower platform was designed to match the acceleration pulse applied to a typical ejection seat base.

Forces and moments were recorded at the base of the specimen at 10 kHz using the load cell. Accelerations of upper and lower platforms were recorded at 10 kHz. Three-dimensional vertebral kinematics were recorded at 1.0 kHz using an eight-camera Vicon system (Vicon Corp., Oxford Metrics Group, Oxford, England). Each vertebra was modeled as a segment in the Vicon Body-Builder (Version 3.55) environment using three noncollinear spherical targets (9.5 mm in diameter), with one target placed in the anterior aspect of the body and one in each transverse process. Targets were attached to vertebrae using 1-mm diameter pins. T12 and L5 targets were glued to the PMMA. Local Cartesian coordinate system origins were defined at mid-height and midwidth along the posterior wall of each vertebral body. The Euler method was implemented to compute three-dimensional orientation of each body in the sequence XYZ. Target motions were used to reconstruct vertebral kinematics. Sagittal segmental angulation

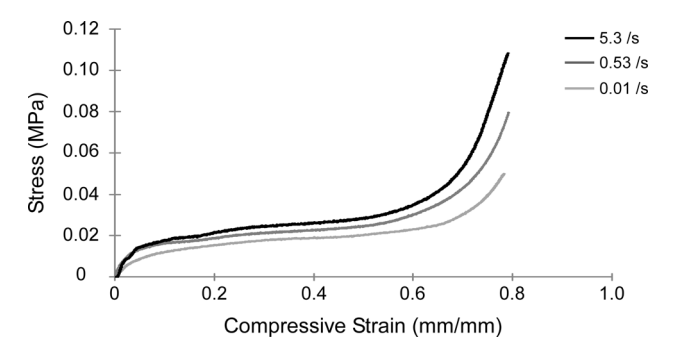


Fig. 2 Compressive mechanical properties of the pulse-shaping foam

was computed for each segment (T12-L1 through L4-L5) as the sagittal plane angle of one vertebra relative to the subjacent vertebra. Additionally, two spherical targets (6.5 mm in diameter) placed in the anterior of each vertebral body (L1 to L4) using 1-mm diameter pins were used to monitor compression of the anterior aspect of each vertebral body. The pins were oriented toward cranial and caudal extents. Vertebral body compression was computed for each level (L1 to L4) as the relative vertical displacement between the two targets within the local axis system.

2.1 Subfailure Tests. The test matrix consisted of two parts. The first part subjected specimens to subfailure loading to outline spinal kinematics and assess repeatability during dynamic vertical deceleration. Subfailure loading was conducted to a maximum acceleration and rate of onset below what was expected to result in soft tissue or bony injury to the spine. This was achieved with a drop height of 61 cm. Mass added to the upper platform (30.2 kg) approximated the thorax, head-neck, and upper extremity mass for a 50th percentile male [26-28]. The mass was added only after the high-power magnet/tension cable was holding the platforms suspended. In this manner, the simulated mass did not compressively preload the specimen. Three subfailure tests were performed for each specimen with the compressive load from the upper platform applied at 1.0, 3.5, and 6.0 cm anterior to the posterior aspect of the L3 vertebral body. These test conditions will be referred to as S1.0, S3.5, and S6.0 from this point forward. Static flexibility tests were performed prior to and following each vertical drop test to identify soft tissue subfailures that may have occurred during dynamic testing. Static flexibility tests consisted of flexing the cranial fixation of the specimen forward using a 5 Nm moment recorded in real-time on the load cell and measuring overall rotation of T12 relative to L5. Shear and axial forces as well as off-axis moments were minimized during this procedure. Preconditioning was not performed as all specimens were dynamically tested and manually manipulated prior to collection of overall T12 to L5 rotation data. Any soft tissue injury would likely be evident by a marked increase in specimen-specific rotation compared to previous flexibility tests. Additionally, X-s were obtained between tests to confirm integrity of the spine (General Electric Healthcare, Milwaukee, WI), and each segment was manipulated by hand to qualitatively assess segmental flexibility.

2.2 Ejection Tests. The second part of the test matrix consisted of acceleration tests designed to induce compression and/or burst fractures as sustained by military pilots during ejection. Each specimen was subjected to an additional test approximating the peak acceleration and rate of onset of the seat base during ejection (Fig. 3). This was achieved with a drop height of 168 cm. Specimens were initially preflexed with a 5 Nm load to bias the results toward an anterior wedge fracture. The upper platform again approximated the mass of the thorax, head-neck, and upper extremities for a 50th percentile male. The anteroposterior location of the loading cylinder from the upper platform was 5 cm anterior to the posterior aspect of the L3 vertebral body. Post-test CT scans were obtained of each specimen in a flexed position to

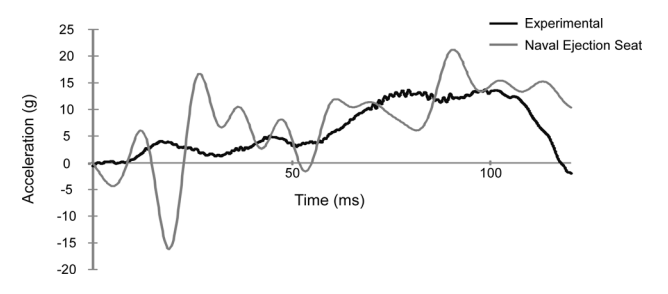


Fig. 3 Vertical acceleration versus time of the lower platform during a simulated ejection test versus acceleration measured during ejection of a Naval ejection seat

Journal of Biomechanical Engineering

AUGUST 2011, Vol. 133 / 081002-3

confirm the presence/absence of vertebral fracture. Because no specimen sustained identifiable injury during the initial ejection tests, one specimen was subjected to two additional tests with identical boundary conditions and increasing peak acceleration and rate of onset. Post-test CT scans were obtained of that specimen in the flexed position following the final test.

2.3 Metrics. Several metrics were quantified during subfailure and ejection tests. Maximum acceleration (g) and rate of acceleration onset (g/s) were used to assess repeatability of the input acceleration pulse between test conditions, and can be used as an estimate of seat-base accelerations during real-world pilot ejections. Rate of acceleration onset was computed as the maximum acceleration divided by the time duration between acceleration onset and the maximum level. Accelerations were filtered according to Channel Frequency Class (CFC) 60 specifications [29]. Axial forces (N) and sagittal plane bending moments (Nm) were recorded using the load cell, inertially compensated, transferred to the posterior aspect of the L5 vertebral body, and filtered according to CFC 600 specifications. Forces and moments were also used to assess repeatability and demonstrate differences between the three subfailure loading conditions. These metrics can also be used as injury tolerance predictors. Vertebral segmental angles (deg) were filtered according to CFC 60 specifications and used to define sagittal plane kinematic differences between the three loading conditions. Vertebral body compressions (mm) were computed as the change in vertical distance between cranial and caudal vertebral body targets and were filtered according to CFC 60 specifications. Because target placements approximated cranial and caudal extents of the body, these data are presented in this manuscript as relative compressions (mm/mm), computed by dividing the change in vertical distance by the initial vertical distance between targets. Relative vertebral body compressions can be used to confirm integrity or identify bony fracture of the body.

3 Results

Mean age, height, and weight of the four male PMHS from which lumbar spines were obtained were 35 ± 8 yrs, 179 ± 7 cm, and 107 ± 7 kg. Each specimen was subjected to four dynamic tests, with one specimen subjected to an additional two tests (total of six) to obtain vertebral fractures. Kinematic data were not collected for one specimen during the S3.5 subfailure test. Therefore, mean kinematic data from the S3.5 condition represent only three specimens.

3.1 Subfailure Tests. Magnitude of peak lower platform vertical accelerations for test conditions S1.0, S3.5, and S6.0 were 6.1 ± 0.4 g, 6.3 ± 0.5 g, and 7.0 ± 0.6 g. Rate of onset for lower platform accelerations for test conditions S1.0, S3.5, and S6.0 were 58.1 ± 10.3 g/s, 55.7 ± 10.2 g/s, and 72.3 ± 4.1 g/s. Maximum compressive forces and bending moments during S1.0, S3.5, and S6.0 tests are summarized in Table 1. A representative time-based loading history of these data is included in Fig. 4.

Table 1 Summary of maximum axial forces (N), bending moments (Nm), and segmental angles (deg) for subfailure testing. Data are presented as mean \pm standard deviation. Negative segmental angle indicates extension; negative axial force indicates compression; negative shear force indicates anterior-posterior shear

S1.0	S3.5	S6.0
-3.3 ± 0.7	5.3 ± 0.6	6.1 ± 2.7
-3.4 ± 0.6	3.6 ± 0.5	4.6 ± 1.1
-2.5 ± 0.5	1.7 ± 2.2	4.8 ± 0.7
-1.9 ± 0.6	-1.5 ± 0.9	1.0 ± 1.6
5.9 ± 0.9	-0.6 ± 2.7	-3.5 ± 0.6
-1874 ± 107	-1868 ± 59	-1865 ± 95
-47 ± 99	-340 ± 86	-603 ± 154
45 ± 3	31 ± 8	21 ± 6
	-3.3 ± 0.7 -3.4 ± 0.6 -2.5 ± 0.5 -1.9 ± 0.6 5.9 ± 0.9 -1874 ± 107 -47 ± 99	$\begin{array}{cccccccccccccccccccccccccccccccccccc$

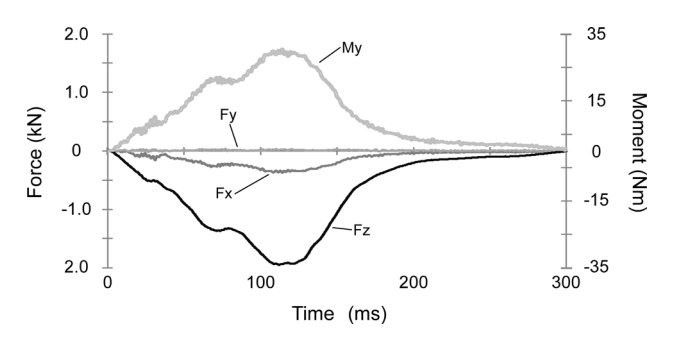


Fig. 4 Representative time-based loading history for test condition S3.5

Segmental kinematics of the lumbar spine demonstrated biphasic curvature during all tests and were dependent upon test conditions (Fig. 5). Condition S1.0 resulted in mean extension at T12-L1 through L3-L4 levels with flexion at the caudal level. However, lumbar spines demonstrated opposite curvature as the load application location was moved ventrally. Condition S3.5 resulted in mean flexion at T12-L1 through L2-L3 levels and condition S6.0 resulted in mean flexion at T12-L1 through L3-L4 levels. Therefore, compressive flexion was well achieved for loading conditions with eccentricities of 3.5 cm and greater. The L4-L5 level extended for both conditions. Specimen-to-specimen repeatability of segmental kinematics was considered to be acceptable.

The possibility of bony fracture or soft tissue injury during subfailure tests was assessed using a number of metrics. Bony fracture was unlikely in any specimen as relative vertebral body compressions varied between 0.2% and 3.3% across all subfailure tests. Post-test inspection of each specimen did not reveal evidence of soft tissue or bony failure. Additionally, static assessment of T12-L5 flexibility also indicated that soft tissue failure during dynamic subfailure testing was unlikely. Prior to dynamic testing, the four specimens flexed an average of 7.7 ± 1.3 deg in response to a 5 Nm flexion moment. For three specimens, overall static T12-L5 flexion varied by less than 12% following the three dynamic tests. In most cases, flexion rotation following dynamic loading increased slightly compared to pretest levels. For the fourth specimen, overall static T12-L5 flexion increased by 21% following the S3.5 test. However, increased flexibility following the S3.5 test for that specimen was likely not indicative of soft tissue failure as flexibility decreased by 13.7% following the subsequent dynamic test (S6.0).

3.2 Ejection Tests. Following subfailure testing, each specimen was subjected to a single test with loading and boundary conditions designed to match the vertical acceleration experienced during pilot ejection. Magnitude of peak lower platform vertical acceleration for the four ejection tests was 14.8 ± 1.7 g. Rate of onset for the four tests was 178.9 ± 11.3 g/s. Maximum compressive forces and flexion moments were -4581 \pm 121 N and 84 \pm 26 Nm. Analysis of vertebral body compressions at L1 through L4 levels during dynamic ejection tests indicated that bony compressive fracture was unlikely in any specimen. Maximum vertebral body compressions did not exceed 4.1% at any spinal level for any of the ejection tests. Three of four specimens demonstrated minimal increases in post-test flexibility compared to baseline tests (1.1% to 15.6%). However, the fourth specimen demonstrated marginally increased T12-L5 rotation (+20%) that is indicative of increased flexibility and may indicate soft tissue failure or subfailure that would have occurred during the previous ejection test. However, specific tissue failure was not identified during post-test inspection of that specimen.

Due to the lack of bony fracture during previous subfailure and ejection tests, one specimen was subjected to two additional tests of increasing acceleration and rate of onset to generate vertebral body compression fracture and validate the clinical relevance of this new experimental model. The chosen specimen demonstrated

081002-4 / Vol. 133, AUGUST 2011

Transactions of the ASME

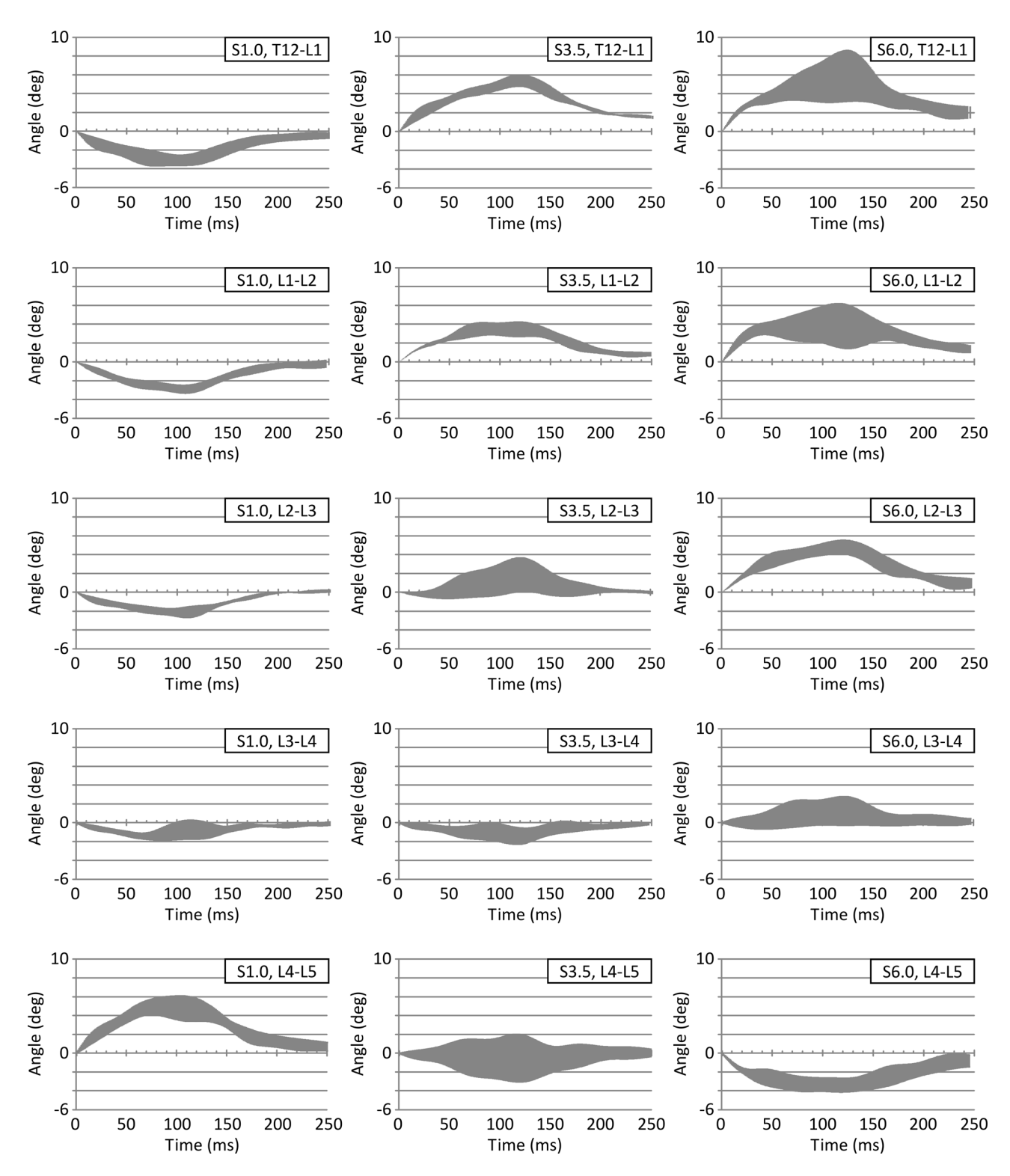


Fig. 5 Segmental kinematics obtained from subfailure testing (flexion: positive; extension: negative). Each column of plots represents a different testing condition with S1.0, S3.5, and S6.0 corresponding to tests with the torso load applied 1.0, 3.5, and 6.0 cm anterior to the posterior aspect of the L3 vertebral body. Kinematic corridors were defined as the mean experimental response ±1 standard deviation.

the smallest increase in flexibility following the previous ejection test (i.e., 1.1%). The first test of increased severity resulted in a lower platform maximum acceleration of 16.4 g with 329 g/s rate of onset. This was achieved by raising the drop height to 198 cm. Post-test inspection did not reveal evidence of bony fracture, although static flexibility increased by 21%, which was slightly greater than average flexibility increases resulting from subfailure

testing. Therefore, the specimen was subjected to a second test of increased severity with maximum acceleration of 21 g and rate of onset of 488 g/s. This was achieved by increasing the stiffness of the pulse-shaping foam while maintaining drop height at 198 cm. Relative vertebral body compressions during that test approached 60% at the L4 level. Compressions at the L2 and L3 levels were less than 20%. Maximum axial force during the last

Journal of Biomechanical Engineering

AUGUST 2011, Vol. 133 / 081002-5

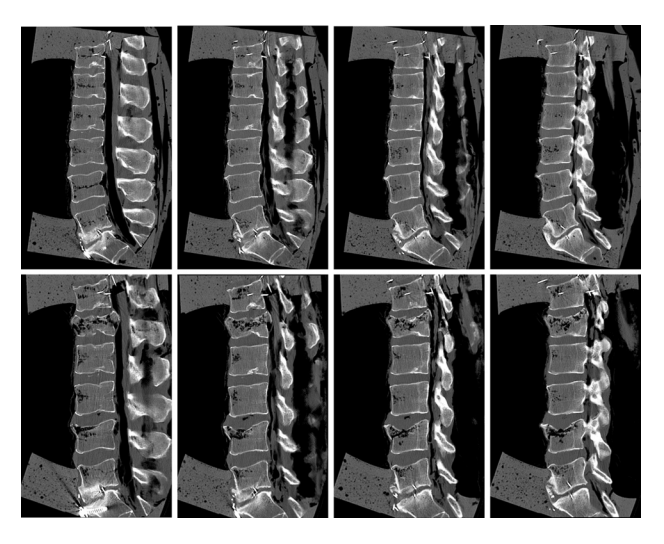


Fig. 6 Sagittal CT of the specimen subjected to higher severity acceleration pulses demonstrating burst fracture at L1 and anterior wedge fracture at L4. Top row images were obtained prior to dynamic testing and bottom row images were obtained immediately following the last test. The two images in each column were obtained from approximately the same medial-lateral position.

increased-severity test was -6106 N, maximum sagittal moment was 168 Nm flexion, and maximum shear force was -1382 N. Posttest CT confirmed the presence of anterior wedge fracture at the L4 vertebral body with loss of integrity for the upper endplate and decreased vertebral body height in the anterior compared to the posterior region (Fig. 6). The post-test CT also confirmed a more traditional burst fracture at L1 with retropulsion of bony fragments into the spinal canal. That fracture was not kinematically identified because the cranial vertebral body target was lost by the Vicon system during the test due to interference with the cranial fixation.

4 Discussion

The present study developed a biomechanically accurate experimental model to investigate lumbar spine injuries during high-rate axial loading. This type of loading can be experienced during pilot ejection from military aircraft, underbody blast due to improvised explosive devices, or falls from height. Loading conditions in this manuscript were biased toward modeling pilot ejection. The model is flexible in terms of applied accelerations/loads and location of load application to the cranial end of the spine. Therefore, the model can induce specimen-specific inertial loading to the spine via the addition of variable mass to the upper platform, can simulate a wide range of loading scenarios by controlling the magnitude and duration of vertical acceleration, as well as the rate of onset, and can model occupants in and out of position (e.g., forward flexed at the time of ejection). Although complex bending occurred due to the extended length of the column, the model demonstrated adequate specimen-to-specimen kinematic repeatability (Fig. 5). Additionally, the wide range of metrics incorporated during model development, including accelerations, loads, segmental kinematics, vertebral body compressions, and pre/post test CT and flexibility measurements, will permit the identification of accurate injury tolerance thresholds for specific loading scenarios during future testing.

Accelerations during the first part of this study were designed to be below the threshold of injury. As such, axial forces and sagittal bending moments were well below previously published thresholds from studies incorporating an MTS piston [18,22,23,30]. Flexibility of the specimens were measured prior to testing and following each dynamic test to ensure that no soft-tissue (or bony) injuries occurred. Increased flexibility following a dynamic test would be indicative of injury. Maintaining that level of increased flexibility following successive tests would confirm

injury. This type of sustained increase in flexibility was not evident for any of the specimens following subfailure tests. Additionally, any isolated flexibility increases were well below increases reported in literature (57% to 123%) for injured spines [31,32]. Therefore, it was concluded that injuries were not sustained by any specimen during subfailure tests. Post-test manipulation and radiography further confirmed the integrity of the spine following all subfailure tests. However, ejection tests were designed to induce clinically relevant injuries and included a 5 Nm flexion preload to bias fractures toward the anterior column. As the spine is flexed, the facet joints bear a lower share of axial loads and stresses increase in the anterior column [33]. Increased anterior column stresses increase intradiscal pressure, augmenting endplate bulging into the cancellous bone and resulting in lower compressive tolerance of the vertebrae [34,35]. Experimental testing has provided support for this assertion, wherein preflexed specimens had lower compressive strength than specimens tested in a neutral posture [11,19,36]. Although spinal posture largely affects the distribution of load among spinal tissues, concurrent dynamic flexion will not change the site of injury from the vertebrae to the intervertebral disc when peak load magnitudes exceed 50% of the local compressive tolerance [37]. Thus, using a preflexed posture for ejection tests in the present study was warranted given the magnitude of compressive loading.

A number of peer-reviewed articles and public-access military reports have reported on the type and rate of injuries sustained during pilot ejection. The rate of severe injuries sustained by pilots during ejections has been cited between 9.3% and 52.1% [38,39]. A majority of serious injuries sustained during ejections were vertebral body fractures, commonly occurring at the thoracolumbar junction [3,7,9,10,40,41]. For example, one study reporting 152 vertebral fractures resulting from 218 ejections indicated that fractures were distributed between T5 and L4 spinal levels, with the maximum number occurring at T11 to L1 [1]. Studies incorporating contemporary ejections reported similar findings [3,6,7,10,41]. Comparable axial loading scenarios produced similar injury outcomes. Axial spinal loading due to helicopter crashes, motor vehicle crashes, parachute jumping, and falls from height produced similar vertebral fracture frequency distributions [42–46]. Therefore, although the injury model was focused on injuries sustained during pilot ejection, the current model can also be used to study other axial loading scenarios since injury patterns are consistent and loading/boundary conditions of the model are flexible.

The present study was focused primarily on model development and demonstration of its repeatability. As such only one specimen was exposed to accelerations sufficient to induce spinal fracture. Nonetheless, the Denis classification scheme was used to categorize the thoracolumbar fractures produced in that specimen [47]. The specimen subjected to higher severity vertical pulses in the current study sustained a type-A burst fracture at L1 (Fig. 6). Loss of integrity occurred for all three columns at that level. Comminution of the entire vertebral body occurred resulting in fracture of both end plates and retropulsion of body fragments into the canal. The left lamina was also fractured (Fig. 7). A type-B compression

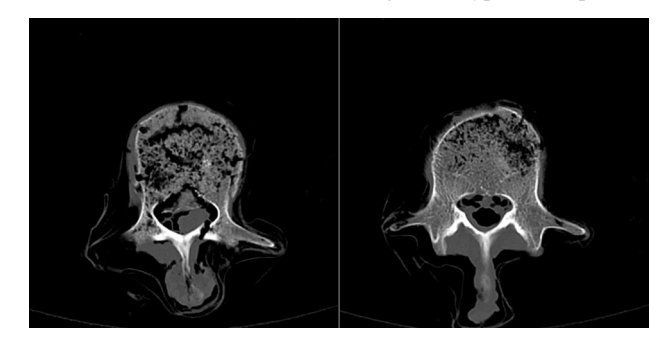


Fig. 7 Axial CT of the specimen subjected to higher severity acceleration pulses demonstrating laminar fracture at L1 (*left*) and intact posterior column at L4 (*right*)

081002-6 / Vol. 133, AUGUST 2011

Transactions of the ASME

fracture was sustained at L4. The mechanism of fracture was anterior flexion, resulting in the most frequent type of compression fracture, failure of the anterior aspect of the upper end plate. The posterior wall of the body, pedicles, and lamina at L4 remained intact (Fig. 7). Therefore, the post-injury sagittal projection of the vertebral body maintained a "wedge" shape with height of the anterior region decreased compared to the posterior region. Clinical studies of pilot ejection have also demonstrated multiple noncontiguous spinal injuries, although specific injury patterns were not described [3,6,7]. Therefore, the clinically relevant injury pattern developed in this study validates the model and forms a basis for continued investigation to define injury tolerance thresholds during high rate vertical accelerations of the lumbar spine.

Although the present model was designed to experimentally recreate the biomechanical effects of pilot ejection on the lumbar spine, some differences from an actual pilot ejection should be noted. The most remarkable difference between this model and a pilot ejection is the duration of the vertical acceleration pulse. The mean experimental ejection pulse was shorter than an acceleration pulse measured on a contemporary Naval ejection seat. While the rate of onset and peak acceleration of the two pulses were approximately equal (Fig. 3), the real world ejection pulse was 2 to 3 times longer, which resulted in an overall displacement of greater than 3 m. The present experimental model was decelerated over less than 65 cm. However, this difference in duration is thought to play a secondary role in the development of vertebral injuries described in this manuscript. Specifically, timing of the L1 burst fracture and L4 wedge fracture indicated that both injuries occurred during the initial acceleration rise. Analysis of the relative vertical displacement for three-vertebrae segments in the upper (T12 to L2) and lower (L3 to L5) lumbar spine during failure tests indicated that maximum upper lumbar vertical displacement was markedly greater than lower lumbar displacement and

attained the maximum value by 35 ms following the onset of acceleration (Fig. 8(a)). If nonfractured vertebral bodies are considered to be rigid, vertical displacement of the L3 to L5 segment would consist primarily of L3-L4 and L4-L5 intervertebral disc deformations. Total deformation of the T12-L1 and L1-L2 discs should be approximately equal. Accordingly, considerably larger segmental vertical displacements in the upper lumbar spine than in lower regions indicates that the L1 burst fracture most likely occurred during this period. Likewise, analysis of anterior vertebral body height change (Fig. 8(b)) indicated that the L4 wedge fracture occurred within the first 44 ms following onset of acceleration. Therefore, this kinematic analysis has demonstrated that lumbar spine injuries sustained using the present experimental model occurred during the initial acceleration rise, which corresponded to the time that the experimental acceleration pulse matched the real-world ejection pulse.

Multiple facets of the present experimental model were novel, although the investigation of axial loading-induced thoracolumbar spine trauma has been experimentally performed in numerous studies. Previous investigations incorporated a variety of human and bovine columns, with loads induced using either a weightdrop technique [13] or MTS piston [22]. The most common model in literature, in terms of the number of specimens tested, has been the three-vertebrae human spine model focusing on T11-L1 or T12-L2 [13,23,24,31,48,49]. Those models typically fixed cranial and caudal vertebrae to focus trauma on the middle vertebra. While useful in defining injury tolerance for specific spinal levels, the approach does not account for the continuous effect of longitudinal ligaments or spinal curvature [50,51]. Both of these factors are likely to influence the uniqueness of lumbar spine trauma under specific loading scenarios [52,53]. Studies incorporating longer spinal segments have typically biased the fracture site by leaving only one level exposed [16,54], similar to three-vertebrae

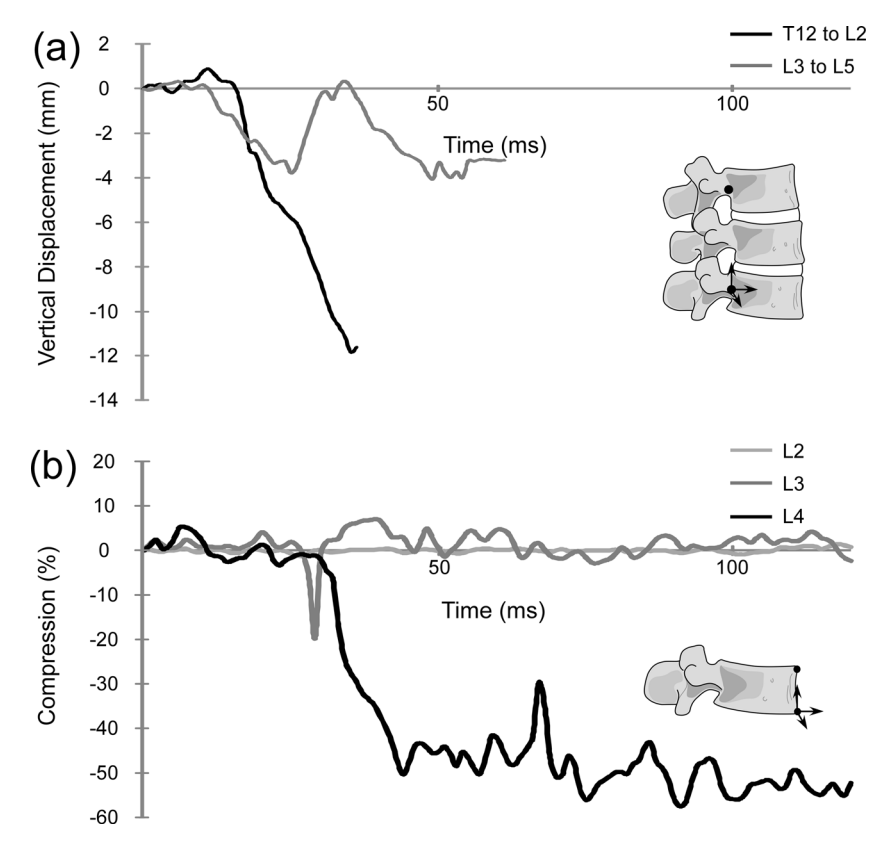


Fig. 8 Time-histories of (a) the relative vertical displacement of three-vertebrae lumbar segments during the injury test (negative: compression), and (b) compression of vertebral bodies during the injury test presented as a percentage of the original displacement between the two targets within the vertebra's local axis system

models, or by creating a stress riser on the anterior cortical shell of one vertebra prior to testing [22,55]. Only two studies performed axial testing of longer columns without biasing the injury site [18,56]. A majority of injuries produced in these two studies were focused in the thoracolumbar region, validating the present injury outcomes.

Historically, the most common model for investigation of thoracolumbar burst fractures due to axial loading has been the weight drop method, as originally published by Willen et al. [13]. Commonly, the metric of interest for injury tolerance in weight drop studies was the impact energy, or simply the potential energy of the falling mass. One study reported an injury threshold of 94.2 J [54]. While impact energy is a useful metric for comparison between weight-drop studies, it has limited application to the investigation of mechanisms or tolerance for real world injuries. Rather, external measures of the realistic loading environment (e.g., acceleration magnitude and rate of onset) or measureable loading quantities (e.g., axial force and sagittal moment) are more applicable to the understanding of injury causation and the development of safer environments for pilots or other humans exposed to high vertical accelerations. As such, the present experimental model was developed to be flexible, enabling the realistic modeling of any number of axial loading scenarios, and to enable measurement of biomechanically relevant metrics. Future application of this model can outline the mechanism of thoracolumbar burst fractures during axial loading, define the method by which biomechanically relevant factors such as age and gender influence injury type and severity, and define realistic tolerance limits for a variety of different loading scenarios (e.g., in and out of position ejections).

Acknowledgment

This research was supported in part by the Office of Naval Research through Naval Air Warfare Center Aircraft Division Contract N00421-10-C-0049 and the Department of Veterans Affairs Medical Research.

References

- [1] Smiley, J. R., 1965, "RCAF Ejection Experience 1952-1961," RCAF Institute of Aviation Medicine, Toronto, Ontario, Report No. AD0465171.
- [2] Smelsey, S. O., 1970, "Study of Pilots Who Have Made Multiple Ejections," Aerosp. Med., 41(5), pp. 563-566.
- [3] Werner, U., 1999, "Ejection Associated Injuries Within the German Air Force From 1981–1997," Aviat. Space Environ. Med., 70(12), pp. 1230–1234. [4] Visuri, T., and Aho, J., 1992, "Injuries Associated With the Use of Ejection
- Seats in Finnish Pilots," Aviat. Space Environ. Med., 63(8), pp. 727–730. [5] Rowe, K. W., and Brooks, C. J., 1984, "Head and Neck Injuries in Canadian
- Forces Ejections," Aviat. Space Environ. Med., 55(4), pp. 313-315. [6] Sandstedt, P., 1989, "Experiences of Rocket Seat Ejections in the Swedish Air Force: 1967–1987," Aviat. Space Environ. Med., 60(4), pp. 367–373.
- [7] Newman, D. G., 1995, "The Ejection Experience of the Royal Australian Air Force: 1951–92," Aviat. Space Environ. Med., 66(1), pp. 45–49.
- [8] Harrison, W. D., 1980, "Ejection Experience in F/FB-111 Aircraft-1967-1978." Proceedings of the Survival and Flight Equipment Association, Annual Symposium, 17th, Las Vegas, NV, Dec. 2-6, 1979, Canoga Park, CA, SAFE Association, Creswell, OR, p. 180-182.
- [9] Hearon, B. F., Thomas, H. A., and Raddin, J. H., Jr., 1982, "Mechanism of Vertebral Fracture in the F/FB-111 Ejection Experience," Aviat Space Environ Med, 53(5), pp. 440-448.
- [10] Lewis, M. E., 2006, "Survivability and Injuries From Use of Rocket-Assisted Ejection Seats: Analysis of 232 Cases," Aviat Space Environ Med, 77(9), pp.
- [11] Panjabi, M. M., Oxland, T. R., Kifune, M., Arand, M., Wen, L., and Chen, A., 1995, "Validity of the Three-Column Theory of Thoracolumbar Fractures. A Biomechanic Investigation," Spine (Phila Pa 1976), 20(10), pp. 1122-1127
- [12] Tran, N. T., Watson, N. A., Tencer, A. F., Ching, R. P., and Anderson, P. A., 1995, "Mechanism of the Burst Fracture in the Thoracolumbar Spine. The Effect of Loading Rate," Spine, 20(18), pp. 1984-1988.
- [13] Willen, J., Lindahl, S., Irstam, L., Aldman, B., and Nordwall, A., 1984, "The Thoracolumbar Crush Fracture. An Experimental Study on Instant Axial Dynamic Loading: The Resulting Fracture Type and Its Stability," Spine, 9(6), pp. 624-631.
- [14] Cain, J. E., Jr., DeJong, J. T., Dinenberg, A. S., Stefko, R. M., Platenburg, R. C., and Lauerman, W. C., 1993, "Pathomechanical Analysis of Thoracolumbar Burst Fracture Reduction. A Calf Spine Model," Spine, 18(12), pp. 1647-1654

- [15] Cotterill, P. C., Kostuik, J. P., Wilson, J. A., Fernie, G. R., and Maki, B. E., 1987, "Production of a Reproducible Spinal Burst Fracture for Use in Biomechanical Testing," J. Orthop. Res., 5(3), pp. 462–465.
- [16] Fredrickson, B. E., Edwards, W. T., Rauschning, W., Bayley, J. C., and Yuan, H. A., 1992, "Vertebral Burst Fractures: An Experimental, Morphologic, and Radiographic Study," Spine, 17(9), pp. 1012–1021.
- [17] Wilcox, R. K., Boerger, T. O., Allen, D. J., Barton, D. C., Limb, D., Dickson, R. A., and Hall, R. M., 2003, "A Dynamic Study of Thoracolumbar Burst Fractures," J. Bone Joint Surg. Am., 85A(11), pp. 2184-2189.
- [18] Duma, S. M., Kemper, A. R., McNeely, D. M., Brolinson, P. G., and Matsuoka, F., 2006, "Biomechanical Response of the Lumbar Spine in Dynamic Compression," Biomed. Sci. Instrum., 42, pp. 476-481.
- [19] Hoshikawa, T., Tanaka, Y., Kokubun, S., Lu, W. W., Luk, K. D., and Leong, J. C., 2002, "Flexion-Distraction Injuries in the Thoracolumbar Spine: An In Vitro Study of the Relation Between Flexion Angle and the Motion Axis of Fracture," J. Spinal Disord. Tech., 15(2), pp. 139-143
- [20] Ochia, R. S., Tencer, A. F., and Ching, R. P., 2003, "Effect of Loading Rate on Endplate and Vertebral Body Strength in Human Lumbar Vertebrae," J. Biomech., 36(12), pp. 1875-1881.
- [21] Shirado, O., Kaneda, K., Tadano, S., Ishikawa, H., McAfee, P. C., and Warden, K. E., 1992, "Influence of Disc Degeneration on Mechanism of Thoracolumbar Burst Fractures," Spine, 17(3), pp. 286-292.
- [22] Yoganandan, N., Larson, S. J., Pintar, F., Maiman, D. J., Reinartz, J., and Sances, A., Jr., 1990, "Biomechanics of Lumbar Pedicle Screw/Plate Fixation in Trauma," Neurosurgery, 27(6), pp. 873-880.
- [23] Langrana, N. A., Harten, R. R., Lin, D. C., Reiter, M. F., and Lee, C. K., 2002, "Acute Thoracolumbar Burst Fractures: A New View of Loading Mechanisms," Spine, 27(5), pp. 498–508.
- [24] Hongo, M., Abe, E., Shimada, Y., Murai, H., Ishikawa, N., and Sato, K., 1999, "Surface Strain Distribution on Thoracic and Lumbar Vertebrae Under Axial Compression. The Role in Burst Fractures," Spine, 24(12), pp. 1197–1202.
- [25] Yoganandan, N., Pintar, F., Sances, A., Jr., Myklebust, J., Schmaltz, D., Reinartz, J., Harris, G., Kalbfleisch, J., Chintapalli, K., and Larson, S., 1988, "Steering Wheel Induced Facial Trauma," 32nd Stapp Car Crash Conference, Atlanta, GA, Society of Automotive Engineers, Inc., Warrendale, PA, pp. 45–69. [26] Damavandi, M., Farahpour, N., and Allard, P., 2009, "Determination of Body
- Segment Masses and Centers of Mass Using a Force Plate Method in Individuals of Different Morphology," Med. Eng. Phys., **31**(9), pp. 1187–1194. [27] Pearsall, D. J., Reid, J. G., and Livingston, L. A., 1996, "Segmental Inertial Pa-
- rameters of the Human Trunk as Determined From Computed Tomography," Ann. Biomed. Eng., 24(2), pp. 198–210.
- [28] Yoganandan, N., Pintar, F. A., Zhang, J., and Baisden, J. L., 2009, "Physical Properties of the Human Head: Mass, Center of Gravity and Moment of Inertia," J. Biomech., 42(9), pp. 1177-1192.
- [29] Society of Automotive Engineers (SAE), 1995, "Instrumentation for Impact Test - Part 1," Society of Automotive Engineers, Warrendale, PA, Report No. SAE J211/1
- [30] Shono, Y., McAfee, P. C., and Cunningham, B. W., 1994, "Experimental Study of Thoracolumbar Burst Fractures. A Radiographic and Biomechanical Analysis of Anterior and Posterior Instrumentation Systems," Spine, 19(15), pp. 1711-1722
- [31] Panjabi, M. M., Oxland, T. R., Lin, R. M., and McGowen, T. W., 1994, "Thoracolumbar Burst Fracture. A Biomechanical Investigation of Its Multidirectional Flexibility," Spine, 19(5), pp. 578-585.
- [32] Panjabi, M. M., Kifune, M., Liu, W., Arand, M., Vasavada, A., and Oxland, T. R., 1998, "Graded Thoracolumbar Spinal Injuries: Development of Multidirectional Instability," Eur. Spine J., 7(4), pp. 332–339.
- [33] Adams, M. A., and Hutton, W. C., 1983, "The Effect of Posture on the Fluid Content of Lumbar Intervertebral Discs," Spine, 8(6), pp. 665–671
- [34] Brinckmann, P., Frobin, W., Hierholzer, E., and Horst, M., 1983, "Deformation of the Vertebral End-Plate Under Axial Loading of the Spine, "Spine, 8(8), pp. 851-856
- [35] Brown, S. H., Gregory, D. E., and McGill, S. M., 2008, "Vertebral End-Plate Fractures as a Result of High Rate Pressure Loading in the Nucleus of the Young Adult Porcine Spine," J. Biomech., **41**(1), pp. 122–127.
- [36] Gunning, J. L., Callaghan, J. P., and McGill, S. M., 2001, "Spinal Posture and Prior Loading History Modulate Compressive Strength and Type of Failure in the Spine: A Biomechanical Study Using a Porcine Cervical Spine Model," Clin. Biomech., 16(6), pp. 471–480.
- [37] Parkinson, R. J., and Callaghan, J. P., 2009, "The Role of Dynamic Flexion in Spine Injury is Altered by Increasing Dynamic Load Magnitude," Clin. Biomech., 24(2), pp. 148-154.
- [38] Nakamura, A., 2007, "Ejection Experience 1956-2004 in Japan: An Epidemiological Study," Aviat. Space Environ. Med., 78(1), pp. 54-58
- [39] Moreno Vazquez, J. M., Duran Tejeda, M. R., and Garcia Alcon, J. L., 1999, "Report of Ejections in the Spanish Air Force, 1979-1995: An Epidemiological and Comparative Study," Aviat. Space Environ. Med., **70**(7), pp. 686–691. [40] Sturgeon, W. R., 1988, "Canadian Forces Aircrew Ejection, Descent, and Land-
- ing Injuries: 1 January 1975-31 December (1987)," Defense and Civil Institute of Environmental Medicine, Downsview, Ontario, Report No. DCIEM No. 88-RRR-56
- [41] Milanov, L., 1996, "Aircrew Ejections in the Republic of Bulgaria, 1953-93," Aviat. Space Environ. Med., 67(4), pp. 364–368.
- Shanahan, D. F., and Shanahan, M. O., 1989, "Injury in U.S. Army Helicopter Crashes October 1979-September (1985)," J. Trauma, 29(4), pp. 415-423.
- [43] Richter, D., Hahn, M. P., Ostermann, P. A., Ekkernkamp, A., and Muhr, G., 1996, "Vertical Deceleration Injuries: A Comparative Study of the Injury

- Patterns of 101 Patients After Accidental and Intentional High Falls," Injury, 27(9), pp. 655-659.
- [44] Hsu, J. M., Joseph, T., and Ellis, A. M., 2003, "Thoracolumbar Fracture in Blunt Trauma Patients: Guidelines for Diagnosis and Imaging," Injury, 34(6), pp. 426–433.
- [45] Inamasu, J., and Guiot, B. H., 2007, "Thoracolumbar Junction Injuries After Motor Vehicle Collision: Are There Differences in Restrained and Nonrestrained Front Seat Occupants?," J. Neurosurg. Spine, 7(3), pp. 311–314.
 [46] Ragel, B. T., Allred, C. D., Brevard, S., Davis, R. T., and Frank, E. H., 2009,
- "Fractures of the Thoracolumbar Spine Sustained by Soldiers in Vehicles Attacked by Improvised Explosive Devices," Spine, 34(22), pp. 2400–2405.
- [47] Denis, F., 1983, "The Three Column Spine and Its Significance in the Classification of Acute Thoracolumbar Spinal İnjuries," Spine, 8(8), pp. 817–831.
- [48] Lin, R. M., Panjabi, M. M., and Oxland, T. R., 1993, "Functional Radiographs of Acute Thoracolumbar Burst Fractures. A Biomechanical Study," Spine, 18(16), pp. 2431-2437.
- [49] Kifune, M., Panjabi, M. M., Arand, M., and Liu, W., 1995, "Fracture Pattern and Instability of Thoracolumbar Injuries," Eur. Spine J., 4(2), pp. 98-103.
- [50] Demetropoulos, C. K., Yang, K. H., Grimm, M. J., Artham, K. K., and King, A. I., 1999, "High Rate Mechanical Properties of the Hybrid III and Cadaveric Lumbar Spines in Flexion and Extension," 43rd Stapp Car Crash Conference,

- San Diego, CA, Society of Automotive Engineers, Inc., Warrendale, PA, pp. 279-294.
- [51] Panjabi, M. M., Crisco, J. J., Vasavada, A., Oda, T., Cholewicki, J., Nibu, K., and Shin, E., 2001, "Mechanical Properties of the Human Cervical Spine as Shown by Three-Dimensional Load-Displacement Curves," Spine, 26(24), pp. 2692-2700.
- [52] Dickey, J. P., and Kerr, D. J., 2003, "Effect of Specimen Length: Are the Mechanics of Individual Motion Segments Comparable in Functional Spinal Units and Multisegment Specimens?," Med. Eng. Phys., 25(3), pp. 221-227.
- [53] Bernstein, M., 2010, "Easily Missed Thoracolumbar Spine Fractures," Eur. J
- Radiol., 74(1), pp. 6–15.
 [54] Panjabi, M. M., Hoffman, H., Kato, Y., and Cholewicki, J., 2000, "Superiority of Incremental Trauma Approach in Experimental Burst Fracture Studies, Clin. Biomech., **15**(2), pp. 73–78.
- [55] Mermelstein, L. E., McLain, R. F., and Yerby, S. A., 1998, "Reinforcement of Thoracolumbar Burst Fractures With Calcium Phosphate Cement. A Biomechanical Study," Spine, 23(6), pp. 664–670. [56] Yoganandan, N., Pintar, F. A., Sances, A., Jr., Maiman, D. J., Myklebust,
- J., Harris, G., and Ray, G., 1989, "Biomechanical Investigations of the Human Thoracolumbar Spine," SAE Trans., 97(5), pp. 676-681.